

Antimicrobial, antioxidant, and cytotoxic activities of endhopitic fungi *Chaetomium sp.* isolated from *Phyllanthus niruri* Linn: in vitro and in silico studies

Rollando^{1,*}, Dion Notario¹, Eva Monica¹, Martanty Aditya¹, Rehmadata Sitepu¹

¹ Program of Pharmacy, Faculty of Science and Technology, Ma Chung University, Malang 65151, Indonesia

*Corresponding email: ro.llando@machung.ac.id

Received 17 January 2017 ; Revised 7 March 2017 ; Accepted 8 March 2017

ABSTRACT

Endophytic fungi *Chaetomium sp.* isolated from *Phyllanthus niruri* Linn. Mycelium powder was extracted by using ethyl acetate. Extract was fractionated using n-hexane, dichloromethane and ethanol 96%. The antimicrobial test was carried out using disc diffusion and microdilution methods. The antioxidant activity of the fraction was determined using hydrogen peroxide free radical scavenging and reducing power capacity activities. The cytotoxicity assay of the fraction against T47D breast cancer cell was carried out using dimethylthiazol-2-yl-2,5-diphenyltetrazolium bromide method (MTT). The in silico prediction of chemical substances which are reported exist in *Chaetomium sp.* performed using AutoDockVina embedded in PyRx version 8.0. Dichloromethane fraction was found as the most active sample against *Escherichia coli* (IC₅₀ 20.76 µg/mL), *Staphylococcus aureus* (IC₅₀ 70.15 µg/mL), *Salmonella typhi* (49.13 µg/mL) and was found as the most high phenolic content with value 47.44 mg GAE/g fraction, whereas the best antioxidant activity was performed by ethanol 96% fraction (85%). Cytotoxicity assay against T47D cell line showed dichloromethane fraction have highest activity with IC₅₀ 10.76 µg/mL. The docking studies showed that compounds bearing xanthone structure were potential for maltose binding periplasmic and human aromatase associating with their potencies as antibacteria and anticancer. Endophytic fungi *Chaetomium sp.* was isolated from *Phyllanthus niruri* using n-hexane, dichloromethane and ethanol fractions was studied its various biological activities as antimicrobial, antioxidant and cytotoxic agent against breast cancer cell.

Key word: Endophytic fungi, *Chaetomium sp.*, *Phyllanthus niruri* Linn, Biological activities, Molecular docking

INTRODUCTION

Endophyte is a microsize particle symbiotically lives in between xylem and phloem, leaves, roots, fruits and stems [1]. Fungal endophyte was known to produce some biological active compounds such as alkaloid, terpenoid, phenolic compounds.[2], working as antioxidant, anticancer, antibacterial, antiviral, antifungal and antileishmanial [3]. Previously, *Phyllanthus amarus* was identified depositing a class of fungi or bacteria named as endophyte, which lives in between plant cells [4]. The fungal endophyte is indicated as much as 10 types in *Phyllanthus amarus* [5], therefore, this herb has been reported as the resource in producing fungal endophyte applied in the development of drug with various biological activities.

The journal homepage www.jpacr.ub.ac.id
p-ISSN : 2302 – 4690 | e-ISSN : 2541 – 0733

In the same family of *Phyllanthaceae*, *Phyllanthus niruri* also has a potential to be a new source for producing fungal endophyte. Originally, this herb contains chemical substances including lignin, glycoside, alkaloid, ellagitannin, terpenoid, phenylpropanoid, flavonoid and polyphenol [6]. Instead of this herb has been studied its pharmacological activity in the treatment of bladder infection, as immunomodulator, anti-inflammatory and antiviral agents [7, 8], to date, there is no report about this species to be used as an endophyte source. Hence, it is interesting to study more about extraction and biological testing of fungal endophyte from *Phyllanthus niruri*.

Resistance in some antimicrobial therapeutics needs a high concern in discovering and developing new antibacterial which are more susceptible to the mutant and selective to eradicate the bacteria cells with no effects to the host [6]. Subsequently, antioxidant currently becomes a hot topic related with oxidative stress associating with cells damage, indicating some diseases such as cancer and coronary heart disorder [9]. Furthermore, the searching of cancer drug that is less toxic has been a lengthy challenge with the results of no anticancer agent is perfectly killing the cancer cells growth without affecting the normal cell [10]. In this present study, we explore the opportunities of *Phyllanthus niruri* as the new source for mining fungal endophyte in organic fractions such as *n*-hexane, dichloromethane and ethanol to be further studied *in vitro* antibacterial, antioxidant and anticancer due to its cytotoxicity effects towards breast cancer cells type T47D.

In rational drug design, the proteins which are responsible towards the pathogenesis can be used as the target in combating the microorganism as well as the malign cells such as tumor. In this study, we have not identified the compounds contained in fungal endophyte of *Phyllanthus niruri* and we also have not tested the fractions against *E. coli* and T47D cells at protein levels due to our limitations. However, we tried to gain an insight mechanism of compounds in the most active fraction by using compounds reported in other *Chaetomium* sp. as the model. In particular, an *in silico* prediction of a possible mechanism as antibacterial and its cytotoxic activity against the breast cancer cell using molecular docking was also discussed.

EXPERIMENT

Chemicals and instrumentation

Phyllanthus niruri leaves were collected from Materia Medica, Malang, Indonesia with specimen code was MN 02371. Potato dextrose broth (PDB) was prepared from potatoes collected from Batu, Malang. Dextrose, muller hinton, potato dextrose agar (PDA), nutrient agar (NA) and nutria broth (NB) were purchased from Merck. The microbes used were *Escherichia coli* (*E. coli*) K-12, *Staphylococcus aureus* (*S. aureus*) NCTC 8325 and *Salmonella typhi* (*S. typhi*) Ty2 purchased from Microbiology Laboratory, Brawijaya University, Indonesia. All chemicals used were analytical grade i.e., ethyl acetate, *n*-hexane, methanol, chloroform, hydrogen peroxide, phosphate buffer pH 7.0, potassium iron (III) cyanide, iron (III) chloride, Thin Layer Chromatography Silica F₂₅₄ plate, and silica 60 for column chromatography were purchased from Merck. T47D cell was courtesy from Parasitology Laboratory of Medical Faculty, Gadjah Mada University, Dulbecco's Modified Eagle Media (DMEM), Fetal Bovine Serum (FBS) 10% (v/v), penicillin-streptomycin, fungizone 0,5% v/v and trypsin-EDTA 0,25% were purchased from Gibco, while Tissue Culture Dish was from Iwaki.

The instruments used are autoclave (AC-300AE, Tiyoda Manufacturing Co. Ltd), shaking incubator, TLC chamber, Laminar Air Flow cabinet (FARRco) and UV-Vis spectrophotometer (Shimadzu).

Tissue culture of endophytic fungi

The colony of endophytic fungi was taken from PDA using ose to have 5 plugs with 0.5 cm in diameter. A volume of 200 mL of the colony was inoculated into a sterilized conical flask and then incubated at room temperature for 14 days. The mycelium was then collected from the filtrate by filtration, followed by drying them at 50°C. Thereafter, the dried mycelium was then pulverized.

Extraction

The mycelium powder was macerated using ethyl acetate (1:3) for 48 hours with a frequent agitation. The liquid extract was then filtrated and the residue was macerated using new ethyl acetate for 24 hours with the same frequent agitation. The filtrate was then collected and concentrated under reduced pressure.

Fractionation

The concentrated extract (200 mg) was then fractionated using 200 mL of each *n*-hexane (100%), dichloromethane (100%) and ethanol 96% through chromatography column with an isocratic technique. Each fraction was collected and concentrated under reduced pressure followed by drying them at 50°C.

Antimicrobial test

The antimicrobial test was carried out using disc diffusion (Kirby-Bauer Test) [11] method whereas the minimum inhibition concentration (MIC) was performed using micro-dilution test [12].

Screening of active fraction

The series of concentration for each fraction was prepared to make 100, 50, 25, 12.5 and 6.25 µg/mL of working solution. Ten µL of each was dropped into paper disc which have amounts of the isolate for each paper disc i.e. 1000, 500, 250, 125 and 62.5 µg/mL and left it to dry leading to the paper disc attachment on the media. Streptomycin 10 mg/mL (10 µL) and a sterile anhydrous ethanol were used as the positive control and the negative control, respectively. The bacterial culture was then incubated at 37°C for 18-24 h followed by viewing the inhibition zone around the paper disc. The larger diameter of the inhibition zone was selected as the active fraction.

Determination of Minimum Inhibition Concentration (MIC)

A volume of 50 µL of Muller Hinton media was transferred into 96-microwell plate, followed by adding 50 µL of bacterial suspension, which have been adjusted its turbidity based on McFarland standard 0.5 [13]. This mixture was then diluted up to 10 times by adding 100 µL of active fraction for each well; therefore, the final concentration would be 250, 125, 62.5, 31.25, 15.63, 7.81, and 1.96 µg/mL. Streptomycin 10 mg/mL was used as the positive control. The sample was then incubated at 37°C for 18-24 h and the cell density was measured as absorbance using microplate reader at 595 nm. The absorbance values were converted into percentage inhibition and then extrapolated against the concentration of the active fraction. The IC₅₀ of the fraction was then calculated and analyzed according to Litchfield dan Wilcoxon method. The MIC measurement was performed by using dropper to take 3 µL of the solution from each well to be streaked on the NA media without adding the microbes and working solution. If only the streaked media being clear after 18-24 h of incubation at 37°C, the MIC value was defined.

Determination of a total phenolic content

The total phenolic content was determined using Folin-Ciocalteu reagent with gallic acid as the reference [14]. Each of fractions was dissolved into methanol which had 2 mg/mL of concentration followed by adding 500 μ L of Folin-Ciocalteu (50%) and 2 mL of Na_2CO_3 20%. This mixture was top up with 5 mL of distilled water and then stored at room temperature for 20 min by maintained its absorbance at 765 nm. The total phenolic content was observed by applying the absorbance value to the linear regression equation generated from the gallic acid standard curve (30; 45; 60; 75; and 90 μ g/mL).

Determination of antioxidant activity

Two methods were used in determining the antioxidant activity of the fraction, i. e., hydrogen peroxide free radical scavenging [3] and reducing power capacity [15].

Hydrogen peroxide free radical scavenging

A solution of hydrogen peroxide (40 mmol/L) was prepared using phosphate buffer pH 7.5. The fraction was dissolved into distilled water to have 2 mg/mL of concentration and then added by H_2O_2 solution. After 10 minutes of reaction, the sample was maintained its absorbance at 230 nm. The capacity of the fraction to scavenge the H_2O_2 radical was calculated based on the formula as followed:

$$\text{Scavenging capacity (\%)} = \left[\frac{A_i - A_t}{A_i} \right] \times 100\%$$

Where A_i = absorbance of the control, A_t = absorbance of the sample.

Reducing power capacity

Each of fractions was dissolved into 1 mL of distilled water and then mixed up with 2.5 mL of phosphate buffer pH 6.6 and 2.5 mL of potassium iron (III) cyanide 1 % w/v. The mixture was then centrifuged at 3000 rpm for 10 min. The upper phase was taken 2.5 mL and then added with another 2.5 mL of distilled water, followed by adding 0.5 mL of FeCl_3 0.1% w/v. The absorbance was then measured at 700 nm using UV spectrophotometer.

Cytotoxicity assay

The cytotoxicity assay of the fraction against T47D breast cancer cell was carried out using (3-(4,5-Dimethylthiazol-2-yl)-2,5-Diphenyltetrazolium Bromide (MTT) method [16]. The T47D cell was cultured on the RPMI media, whereas the normal cell (Vero) was cultured on the M199 media. Each of them contained FBS 10%, penicillin-streptomycin 1% and fungizone 0.5%. A series of working solution was prepared with concentrations as followed: 7.81, 15.62, 31.25, 62.5, 125, 250 and 500 μ g/ml. Cisplatin (15 μ M) was used as the positive control. The cell viability was determined at 595 nm and the absorbance was converted into the percentage viability using plate reader. The IC_{50} was calculated by plotting the % viability against the concentration of the fraction and the selectivity index (SI) was defined according to the ratio between the IC_{50} of Vero cell and the IC_{50} of T47D cell.

Molecular Docking

The in silico prediction of chemical substances which are reported presenting in *Chaetomium* sp. from diverse plants regarding with their activities against the selected bacteria and T47D cells were carried out by docking the compounds into 10 representative protein targets from the selected bacteria and T47D cells, respectively. The ligands were sketched and geometrically minimized using ACD ChemsSketch (www.acdlabs.com) and Marvin Sketch (www.chemaxon.com), respectively. The ligands and proteins were then

prepared using AutoDockTools 1.5.6 (www.autodock.scripps.edu). The proteins were added with polar hydrogen and given by kollman charge whereas the ligands were given by gasteiger charges. The grid was centered on each protein binding site and the docking was then performed using AutoDock Vina embedded in PyRx version 8.0 (www.autodock.scripps.edu). The docking results were observed as free energy of binding (ΔG_{bind}) and the selected docking pose was visualized using Discovery Studio 3.5 (www.accelrys.com).

RESULT AND DISCUSSION

Fungal endophyte culture

Fungal endophyte of *Chaetomium* sp. (Fig. 1a) which was isolated from *Phyllanthus niruri* leaves, characterized as white fungal colony (Fig. 1b). The fungal morphology was identified by Mycology Laboratory, Agriculture Faculty of Gadjah Mada University, Indonesia. Genus *Chaetomium* sp. had characteristics as followed: a helix solid mycelium, composed of dark hyphae pigment and had uniform sclerotia. These characters were in agreement with fungal endophyte from genus *Chaetomium* sp., which was reported by Sharma [17].

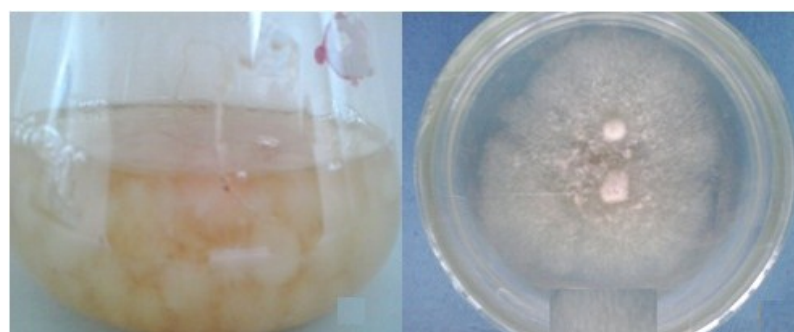


Figure 1. (a) Fungal culture of *Chaetomium* sp. in 14th day of incubation and (b) the morphology of *Chaetomium* sp. with 7 days in age

Screening of active fraction

The preliminary determination of antibacterial activity of the fractions was necessary to select which fraction would be potential for further testing. Table 1 presented the inhibition zone of three fractions (*n*-hexane, dichloromethane and ethanol 96%) towards *S. aureus*, *E. coli* dan *S. typhi*.

Table 1. The results of the disc diffusion assay of the fractions against the bacteria

Fraction	Loading (μg)	Zone of inhibition (mm)(mean \pm SD) $n = 5$ experiments				
		<i>S. aureus</i>	<i>E. coli</i>	<i>S. typhi</i>	(+) control	(-) control
<i>n</i> -hexane	62.5	ND	ND	ND		
	125	ND	ND	ND		
	250	ND	ND	ND	26.3 \pm 0.45	ND
	500	10.5 \pm 0.16	ND	5.2 \pm 0.42		
	1000	7.1 \pm 0.11	8.1 \pm 0.34	6.4 \pm 0.76		

dichloromethane	62.5	2.3±0.19	ND	2.6±0.85		
	125	3.4±0.10	5.1±0.91	3.5±0.44		
	250	6.1±0.78	6.3±0.13	5.6±0.14	21.4±0.45	ND
	500	8.3±0.87	10.3±0.19	7.8±0.39		
	1000	15.5±0.76	12.3±0.76	14.3±0.55		
ethanol 96%	62.5	ND	ND	ND		
	125	ND	ND	ND		
	250	ND	ND	ND	19.1±0.55	ND
	500	ND	2.3±0.45	8.3±0.35		
	1000	3.7±0.93	3.1±0.33	10.5±0.94		

ND: not detected, SD: Standard deviation, *S. aureus*: *Staphylococcus aureus*, *E. coli*: *Escherichia coli*, *S. typhi*: *Salmonella typhi*

As results, dichloromethane fraction demonstrated a higher inhibition towards the bacterial growth than other two fractions. In the lowest concentration (62.5 µg/mL), dichloromethane fraction inhibited *S. aureus* and *S. typhi*, respectively; while neither *n*-hexane nor ethanol 96% fractions performed the inhibitions. The inhibition of all bacteria by dichloromethane fraction was observed at concentration 125 µg/mL, thereafter, the inhibition was proportionally increased along with the higher concentration of the fraction. Towards this fraction, all bacteria are similarly susceptible as shown by its close values of inhibition zone starting from 125 to 1000 µg/mL. On the other hand, *n*-hexane and ethanol 96% fractions were more likely susceptible towards *E. coli* and *S. typhi*, respectively, as shown by its higher inhibitions at 1000 µg/mL. Although they can strongly inhibit the bacteria at the highest concentration only, however, we decided to include them for further IC₅₀ calculation due to its potential selective antimicrobial activity to more specific bacteria as discussed.

Minimum Inhibition Concentration (MIC) and IC₅₀ calculation

The potent fraction was justified from its capability to inhibit the bacteria at the minimum concentration. When the fraction was able to inhibit at least 50% of bacterial growth, only the IC₅₀ value would be defined. Table 2 presented the MIC and IC₅₀ value of each fraction against three bacteria. According to the susceptibility, the dichloromethane was the best fraction due to its capability to inhibit all bacteria at lower concentration than two other fractions.

Table 2. The IC₅₀ and MIC value of three fractions against *S. aureus*, *E. coli* and *S. typhi*

Bacteria	Samples(mean ± SD) n = 5 experiments					
	<i>n</i> -hexane		dichloromethane		ethanol 95%	
	IC ₅₀ (µg/mL)	MIC (µg/mL)	IC ₅₀ (µg/mL)	MIC (µg/mL)	IC ₅₀ (µg/mL)	MIC (µg/mL)
<i>E. coli</i>	124.88±0.34	>500	20.76±0.56	125	101.54±0.87	>500
<i>S. aureus</i>	233.86±0.98	>500	70.15±0.87	250	118.09±0.88	>500
<i>S. typhi</i>	101.98±0.23	>500	49.13±0.55	125	88.12±0.46	>500

SD: Standard deviation, *E. coli*: *Escherichia coli*, *S. aureus*: *Staphylococcus aureus*, *S. typhi*: *Salmonella typhi*, IC₅₀=Inhibition concentration 50%, MIC = Minimum inhibition concentration.

The dichloromethane fraction has less than 100 µg/mL of IC₅₀ to all bacteria indicating its broad spectrum as antibacteria. *E. coli* was the most susceptible bacteria towards the

dichloromethane fraction as it showed the lowest IC₅₀ value (20.76 µg/mL) among three bacteria. Either *n*-hexane or ethanol 96% was less sensitive than dichloromethane, as shown by its IC₅₀ value with more than 100 µg/mL. However, as indicated in the preliminary antibacterial assay, ethanol 96% fraction selectively inhibited *S. typhi* more than other bacteria due to its IC₅₀ value i.e., 88.12 µg/mL, which was potential for a narrow spectrum antibacterial. The least susceptible fraction was detected on *n*-hexane that showed more than 100 µg/mL of IC₅₀ to all bacteria.

The total phenolic content

The total phenolic content is associated with the reducing capacity of the compounds under redox reaction. Table 3 presented the total phenolic content of the three fractions which was found in a quite broad range. Due to its polar character, phenolic compounds were more soluble in a polar solvent such as ethanol 96% than in a semipolar (dichloromethane) and nonpolar (*n*-hexane) solvents. However, in the dichloromethane, the total phenolic content was quite high that might be contributing in the bacterial growth inhibition as known that phenol could denature the protein structure leading to bacterial eradication [18].

Table 3. The total phenolic content of fractions

Fraction	Total phenolic content (mg GAE/g fraction) (mean ± SD) <i>n</i> = 5 experiments
<i>n</i> -hexane	10.11 ± 0.43
dichloromethane	47.44 ± 0.11
ethanol 96%	63.45 ± 0.87

SD: Standard deviation, mg GAE/g fraction: Miligram gallic acid equivalent per gram fraction

Antioxidant activity

Hydrogen peroxide is rapidly decomposed into oxygen and water, which may form hydroxyl radical that can modulate the lipid peroxidation process leading to the cell damage. From this assay, all fractions possessed the free radical scavenging activity at 34-85% (Fig. 2a).

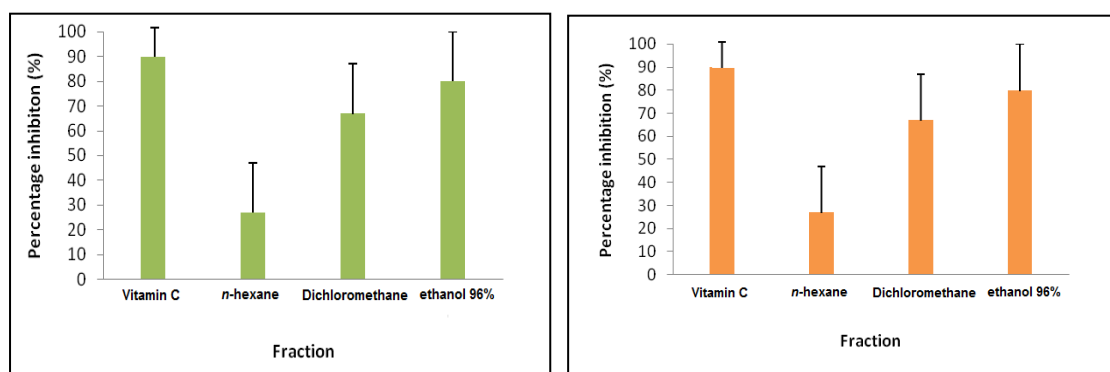


Figure 2. The antioxidant activity of three fractions using methods of (a) H₂O₂ free radical scavenging and (b) reducing power capacity, *n* = 5 experiments

Among the fractions, ethanol 95% demonstrated the highest radical scavenging (85%) which was almost comparable with vitamin C (95%) as the positive control. This was in agreement with the reducing power capacity assay (Fig. 2b) which demonstrated the same

order among the three fractions. The ethanol 96% fraction was able to reduce the reduction of Fe (III) to Fe (II) in such a way those compounds donated electron to stabilize the radicals up to 80% in the ethanol, which was almost compare to that vitamin C (90%) as the positive control. These two antioxidant activities corresponded to the total phenolic content, in which ethanol as a polar solvent able to fractionate phenolic based compounds. This might possess the antioxidant activity associating with lipid peroxidation inhibition.

Cytotoxicity assay against T47D breast cancer cells

T47D is a breast cancer cell lines that is primarily used in breast cancer research [19]. The inhibition of this cell line up to 50% was associated with the potential anticancer from the fractions (Table 4). All fractions were observed IC_{50} less than 100 $\mu\text{g/mL}$ indicating its potential as anticancer with dichloromethane fraction re-showing the lowest IC_{50} value than two others. Fortunately, this fraction showed the highest selectivity index (SI) indicating its selectivity was more to cancer than the normal cell. There have been an agreement between antibacteria and cytotoxicity assay, hence, this fraction was promiscuous for chemotherapeutics against bacteria and cancer cell.

Table 4. The results of cytotoxicity assay against T47D and Vero cell line

Fraction	Samples (mean \pm SD) $n = 5$ experiments		
	IC_{50} T47D($\mu\text{g/mL}$)	IC_{50} Vero($\mu\text{g/mL}$)	SI
<i>n</i> -hexane	122.64 \pm 0.76	253.88 \pm 1.65	2.07
dichloromethane	10.76 \pm 0.23	221.77 \pm 0.96	20.61
ethanol 96%	57.16 \pm 2.34	323.77 \pm 1.65	5.66

SD: Standard deviation, IC_{50} =Inhibition concentration 50%, SI : Selectivity index

The morphology of T47D upon dichloromethane exposure was observed altering the cell being shrunk, died, and reduced in the cell number. These effects were verified by comparing them with the negative control, in which the cell without treatment had no morphology alteration (Fig. 3a-c). The cytotoxic effect of dichloromethane fraction towards Vero cells based on IC_{50} value as well as morphology profile showed the milder effect than T47D cells. However, the dichloromethane fraction exposure altered the morphology of the Vero cell to be shrinking, circling, and detaching from the bottom of the well although it needed more concentration to give the same effect with that of T47D (Fig. 3d-f).

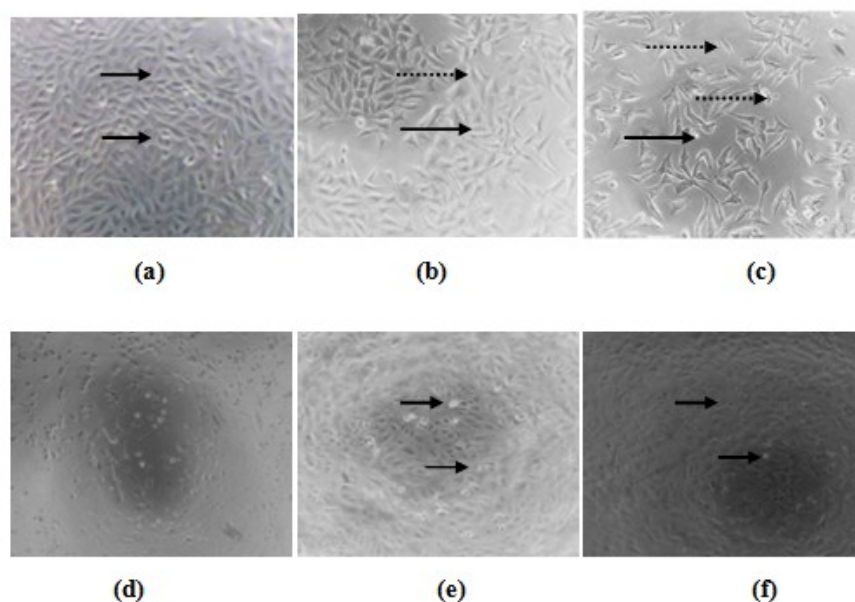


Figure 3. The effect of dichloromethane fraction towards T47D (a-c) and Vero cells (d-f). The viewing was performed under inverted microscope with 100x of magnitudes. (a) negative control (b) dichloromethane fraction 5 $\mu\text{g/mL}$, (c) dichloromethane 10 $\mu\text{g/mL}$, (d) negative control, (e) dichloromethane fraction 250 $\mu\text{g/mL}$ and (f) dichloromethane fraction 500 $\mu\text{g/mL}$. The arrow indicated the living cell whereas the dashed arrow indicated the morphological alteration

In silico prediction of compounds in *Chaetomium* sp. using molecular docking

In silico activity against protein targets in *E. coli*

There have been more than 4,000 open reading frames (ORFs) characterized in the *E. coli* genome, encodes approximately 70% of protein remains in cytoplasm [20]. Ten of them were used as the representative target to study the molecular mechanism of 27 ligands of *Chaetomium* fungal endophyte from diverse plants [21-27]. On the other hand, the proteins being used as the target are methylerythritol phosphate cytidyltransferase (PDB 1I52) [28], maltose binding periplasmic protein (MBP; PDB 1JVV) [29], glutamine-fructose-6-phosphate aminotransferase (PDB 1MOS) [30], γ -aminobutyrate aminotransferase (PDB 1SZS) [31], DNA gyrase (PDB 4DUH) [32], enoylreductase (PDB 1I30) [33], isoleucyl t-RNA synthetase (PDB 1JZQ) [34], aspartate aminotransferase (PDB 1IX6) [35], acetylglutamate kinase (PDB 1OHA) [36], and peptidyl t-RNA hydroxylase (PDB 2PTH) [37]. Table 5 presented the docking results of 26 ligand identified in *Chaetomium* sp. against diverse protein targets in *E. coli*.

Table 7. The $\Delta G_{\text{binding}}$ of 27 ligands were docked into proteins in & T47D cell lines

Ligands	ΔG_{bind} (Kcal/mol) samples (mean \pm SD) <i>n</i> = 10 experiments	1SAO	1W6K	3BBI	3EQM	3G5D	1GWQ	1FM6	3ERT	3HEG	1YSI
HWergos	-8.1 \pm 0.98	-11.2 \pm 0.11	-10.7 \pm 0.76	-10.0 \pm 0.65	-8.6 \pm 0.65	-6.4 \pm 0.85	-7.5 \pm 0.65	-5.8 \pm 0.76	-7.8 \pm 0.98	-7.6 \pm 0.98	-7.9 \pm 0.87
HWergos58	-8.0 \pm 0.65	-9.1 \pm 0.13	-8.4 \pm 0.55	-9.7 \pm 0.99	-8.4 \pm 0.89	-6.4 \pm 0.86	-7.9 \pm 0.99	-5.7 \pm 0.43	-6.9 \pm 0.85	-6.9 \pm 0.85	-7.9 \pm 0.87
Latef1	-8.6 \pm 0.87	-10.1 \pm 0.46	-8.9 \pm 0.63	-9.3 \pm 0.12	-9.3 \pm 0.75	-8.9 \pm 0.98	-8.1 \pm 0.73	-8.8 \pm 0.54	-8.0 \pm 0.77	-8.6 \pm 0.94	-8.6 \pm 0.94
Latef2	-4.8 \pm 0.45	-4.9 \pm 0.63	-4.6 \pm 0.87	-5.8 \pm 1.23	-4.2 \pm 0.43	-4.7 \pm 0.53	-4.3 \pm 0.54	-4.8 \pm 0.76	-4.6 \pm 0.76	-4.6 \pm 0.76	-4.5 \pm 0.48
Latef3	-5.3 \pm 0.37	-5.7 \pm 0.46	-5.1 \pm 0.88	-5.6 \pm 0.35	-4.7 \pm 0.78	-5.5 \pm 0.65	-4.8 \pm 0.48	-5.7 \pm 0.77	-4.8 \pm 0.47	-4.8 \pm 0.47	-5.1 \pm 0.99
Latef4	-8.7 \pm 0.37	-11.3 \pm 0.56	-9.5 \pm 0.97	-9.8 \pm 0.62	-9.8 \pm 0.66	-8.1 \pm 0.77	-7.9 \pm 0.47	-7.3 \pm 0.83	-8.3 \pm 0.85	-8.3 \pm 0.85	-9.6 \pm 0.32
Latef5	-8.5 \pm 0.77	-11.0 \pm 0.66	-9.2 \pm 0.13	-9.6 \pm 0.98	-8.8 \pm 0.62	-8.4 \pm 0.84	-7.8 \pm 0.49	-7.5 \pm 0.99	-8.4 \pm 0.85	-8.4 \pm 0.85	-9.4 \pm 0.66
Latef6	-8.8 \pm 0.98	-10.3 \pm 0.68	-9.0 \pm 0.53	-8.8 \pm 0.77	-9.0 \pm 0.98	-8.7 \pm 0.57	-7.9 \pm 0.77	-8.4 \pm 0.98	-8.0 \pm 0.21	-8.8 \pm 0.53	-8.8 \pm 0.53
Marwah1	-8.0 \pm 0.59	-9.9 \pm 0.31	-8.8 \pm 0.74	-8.3 \pm 0.64	-7.7 \pm 0.88	-6.0 \pm 0.88	-7.2 \pm 0.92	-6.7 \pm 0.83	-7.5 \pm 0.74	-9.3 \pm 0.75	-9.3 \pm 0.75
Marwah2	-7.4 \pm 0.37	-10.6 \pm 0.44	-6.9 \pm 0.77	-8.6 \pm 0.88	-7.3 \pm 0.43	-5.6 \pm 0.72	-7.3 \pm 0.47	-5.8 \pm 0.76	-6.8 \pm 0.64	-8.2 \pm 0.87	-8.2 \pm 0.87
Marwah3	-8.1 \pm 0.87	-3.1 \pm 0.35	-5.8 \pm 0.98	-9.5 \pm 0.82	-8.0 \pm 0.88	-2.0 \pm 0.68	-7.5 \pm 0.83	-1.1 \pm 0.53	-6.3 \pm 0.42	-3.1 \pm 0.74	-3.1 \pm 0.74
Marwah4	-6.9 \pm 0.98	-4.4 \pm 0.51	-8.5 \pm 0.91	-11.3 \pm 0.76	-8.0 \pm 0.43	-1.1 \pm 0.98	-8.0 \pm 0.77	-1.2 \pm 0.65	-7.0 \pm 0.89	-2.8 \pm 0.86	-2.8 \pm 0.86
Marwah5	-6.0 \pm 0.57	-7.8 \pm 0.47	-6.8 \pm 0.65	-6.4 \pm 0.85	-6.2 \pm 0.83	-5.8 \pm 0.92	-5.6 \pm 0.82	-6.3 \pm 0.77	-6.6 \pm 0.66	-7.0 \pm 0.42	-7.0 \pm 0.42
Marwah6	-6.0 \pm 0.98	-8.0 \pm 0.55	-6.0 \pm 0.66	-6.7 \pm 0.44	-5.9 \pm 0.76	-6.0 \pm 0.68	-5.0 \pm 0.39	-6.4 \pm 0.97	-6.7 \pm 0.86	-6.2 \pm 0.46	-6.2 \pm 0.46
Marwah7	-5.2 \pm 0.54	-10.2 \pm 0.73	-7.9 \pm 0.89	-8.4 \pm 0.32	-8.1 \pm 0.77	-6.4 \pm 0.64	-6.9 \pm 0.46	-7.2 \pm 0.86	-6.8 \pm 0.74	-7.0 \pm 0.87	-7.0 \pm 0.87
PengLi	-5.3 \pm 0.49	-6.5 \pm 0.87	-5.9 \pm 0.99	-5.6 \pm 0.94	-6.0 \pm 0.86	-5.9 \pm 0.58	-5.1 \pm 0.74	-6.1 \pm 0.89	-5.7 \pm 0.89	-6.1 \pm 0.88	-6.1 \pm 0.88
Qin1	-0.6 \pm 0.72	-8.7 \pm 0.81	-9.2 \pm 0.42	-9.9 \pm 0.64	-9.3 \pm 0.46	-6.5 \pm 0.88	-8.6 \pm 0.68	-6.2 \pm 0.66	-8.3 \pm 0.76	-9.5 \pm 0.45	-9.5 \pm 0.45
Qin2	0.8 \pm 0.56	-8.5 \pm 0.67	-9.1 \pm 0.64	-9.7 \pm 0.77	-9.2 \pm 0.67	-5.3 \pm 0.94	-8.8 \pm 0.85	-6.1 \pm 0.42	-8.3 \pm 0.43	-9.5 \pm 0.55	-9.5 \pm 0.55
Qin3	-3.5 \pm 0.47	-3.1 \pm 0.82	-9.4 \pm 0.91	-10.0 \pm 0.85	-9.4 \pm 0.53	-6.9 \pm 0.95	-7.9 \pm 0.83	-8.7 \pm 0.52	-10.3 \pm 0.5	-9.4 \pm 0.75	-9.4 \pm 0.75
Qin4	8.8 \pm 0.73	-2.3 \pm 0.44	-10.4 \pm 0.65	-9.1 \pm 0.78	-9.7 \pm 0.24	-5.7 \pm 0.45	-9.0 \pm 0.57	-6.9 \pm 0.68	-10.4 \pm 0.7	-9.7 \pm 0.87	-9.7 \pm 0.87
Wang1	-6.9 \pm 0.84	-10.4 \pm 0.87	-8.5 \pm 0.76	-9.4 \pm 0.96	-9.1 \pm 0.36	-6.5 \pm 0.87	-7.7 \pm 0.52	-5.5 \pm 0.75	-8.2 \pm 0.64	-8.7 \pm 0.86	-8.7 \pm 0.86
Wang2	-5.8 \pm 0.05	-10.0 \pm 0.84	-9.3 \pm 0.77	-9.1 \pm 0.82	-9.7 \pm 0.46	-5.7 \pm 0.98	-8.1 \pm 0.83	-6.3 \pm 0.64	-8.1 \pm 0.86	-9.4 \pm 0.32	-9.4 \pm 0.32
Wang3	-8.4 \pm 0.73	-9.8 \pm 0.99	-8.5 \pm 0.93	-8.0 \pm 0.56	-8.6 \pm 0.66	-8.4 \pm 0.67	-7.2 \pm 0.84	-8.7 \pm 0.55	-8.2 \pm 0.66	-8.6 \pm 0.65	-8.6 \pm 0.65
Wang4	-8.4 \pm 0.57	-9.8 \pm 0.75	-8.8 \pm 0.45	-8.1 \pm 0.81	-8.7 \pm 0.47	-7.9 \pm 0.84	-7.2 \pm 0.83	-8.2 \pm 0.31	-8.4 \pm 0.53	-8.6 \pm 0.76	-8.6 \pm 0.76
Wang5	-6.8 \pm 0.76	-8.2 \pm 0.50	-6.7 \pm 0.65	-6.8 \pm 0.22	-7.0 \pm 0.37	-7.0 \pm 0.89	-6.0 \pm 0.87	-7.0 \pm 0.74	-7.0 \pm 0.68	-7.1 \pm 0.87	-7.1 \pm 0.87
WP1	5.6 \pm 0.86	3.8 \pm 0.63	-6.6 \pm 0.72	-8.9 \pm 0.46	-7.2 \pm 0.36	-3.9 \pm 0.99	-7.4 \pm 0.83	-4.1 \pm 0.52	-7.1 \pm 0.77	-3.6 \pm 0.88	-3.6 \pm 0.88
WP2	7.9 \pm 0.54	7.7 \pm 0.77	-7.2 \pm 0.77	-8.9 \pm 0.71	-6.3 \pm 0.48	-3.8 \pm 0.24	-7.8 \pm 0.65	-4.1 \pm 0.67	-7.4 \pm 0.86	-5.9 \pm 0.98	-5.9 \pm 0.98
Mean	-4.8 \pm 0.25	-7.2 \pm 0.52	-8.0 \pm 0.32	-8.6 \pm 0.62	-7.9 \pm 0.66	-6.1 \pm 0.54	-7.2 \pm 0.84	-6.3 \pm 0.88	-7.5 \pm 0.68	-7.5 \pm 0.93	-7.5 \pm 0.93

ΔG_{bind} : Free energy of binding, 1SAO: Human tubulin cholicine receptor, 1W6K: Human oxydosoqualenecyclase, 3BBI: Erb tyrosine kinase, 3EQM: Human placental aromatase, 3G5D: C-src tyrosine kinase, 1GWQ: Estrogen receptor DNA binding protein, 1FM6: PPR γ nuclear, 3ERT: ER α nuclear receptor, 3HEG: P38 α MAP kinase, 1YSI: BCL-XI.

As results, active ligands showed free energy of binding at range of -12.1 to -3.9 kcal/mol while inactive ligands were found at -0.7 to 7.9 kcal/mol. The positive value of inactive ligands indicated no-affinity between ligand and the protein target in *E. coli*. According to the mean of the ΔG_{bind} , the lowest free energy of binding went to the interaction between maltose binding periplasmic (MBP) protein and the ligand, indicated its strongest binding interaction among 10 protein targets. Maltose binding periplasmic was a huge bacterial periplasmic protein (370 amino acid residues) involved in active transport and chemotaxis towards maltose. This enzyme worked under substantial conformational changes to let maltose binds to the ATP –binding cassette (ABC)-7 transporter, initiating downstream signaling for either transport or chemotaxis [38]. Therefore, the MBP could be the selected protein target for further study. Table 6 presented the amino acid residues involved in the binding of 27 ligands.

Table 6. The amino acid residues identified from the interaction of 27 ligands with 1VY

Ligands	Amino acid residues	Ligands	Amino acid residues
Control	Lys15, Arg66, Tyr155, Asp65, Glu153, Asp14, Glu111	Marwah6	Asn12
HWergos	No H-bond	Marwah7	Asn12
HWergos58	No H-bond	PengLi	Asp65
Latef1	Arg345, Glu44,	Qin1	No H-bond
Latef2	Trp62, Arg66	Qin2	No H-bond
Latef3	Trp62, Arg66	Qin3	Lys42
Latef4	Asn12	Qin4	Lys42, Tyr210, Ser211
Latef5	Asn12	Wang1	Glu153, Lys42
Latef6	Arg345, Glu153	Wang2	Glu153
Marwah1	Lys42	Wang3	Tyr155, Arg66, Arg345
Marwah2	Asn12, Lys15	Wang4	Arg66, Glu111
Marwah3	Asn12	Wang5	No H-bond
Marwah4	Lys42, Leu43, Arg66, Ser211	WP1	Asn12
Marwah5	No H-bond	WP2	Asn12

1JVY: Maltose binding periplasmic protein, Lys: Lysine, Arg: Arginine, Tyr: Tyrosine, Asp: Aspartic acid, Glu: Glutamic acid, Trp: Typtophan, Asn: Aspagine, Leu: Leucine, Ser: Serine, No H-bond: No hydrogen bond

From these 27 ligands, 20 of them were characterized hydrogen bond interaction with MBP, whereas the remained six ligands were absent. The absent hydrogen bond interaction might be due to the nonpolar characters of the ligands bearing steroid, pentadienylfuranol, azaphilone and chromone (Supplementary data table 1), therefore, the ΔG_{bind} of those compounds were significantly contributed by hydrophobic and other van der waals interactions. It is well studied that the strength of van der waals interaction is weaker than hydrogen bond interaction due to their distance bonds, i.e. $> 2.2 \text{ \AA}$ and $1.5 - 2.2 \text{ \AA}$, respectively [39].

Among 20 ligands that interacted with MBP via hydrogen bond interaction, 10 of them demonstrated the binding mode similar to that of control ligand (maltose) indicating their potential to be developed as novel MBP inhibitors. The residues being identified in their binding mode were Lys15, Asp65, Arg66, Glu111, Glu153, and Tyr155. Most of them had one interaction only with the residues, which was also shown by the positive control. However, Wang3 and Wang4 were identified possessing two hydrogen bond interactions

with same residues of the positive control associating with its more potential ligands to be optimized as MBP inhibitors. Figure 4 illustrated the superposition of 27 ligands at the binding site of MBP and the most active ligand-MBP molecular interaction.

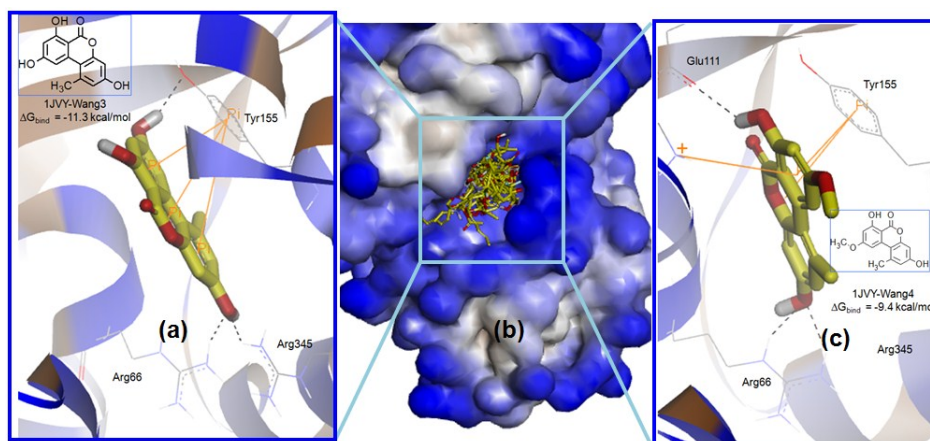


Figure 4. The pose of (a) Wang3, (b) the superposition of 27 ligands in *Chaetomium* sp., and the pose of (c) Wang4 at the binding site of 1JVY. The individual poses of Wang3 and Wang4 was visualized as stick forms with carbon in yellow and standard colors of O and H whereas the protein was performed in ribbon, whereas the superposition was as surface. The protein was colored representing blue as hydrophobic region, brown as hydrophilic region and white as neutral region. The picture was visualized using Discovery Studio 3.5 (www.accelrys.com)

As visualized in Fig. 4a and 4c, Wang3 and Wang4 showed the similar binding mode towards MBP. On one hand, Wang3 showed hydrogen bond interaction with Arg66, Tyr155 and Arg345 and its pose was strongly supported by π - π interaction between three aromatic rings of the ligand with the phenol moiety of Tyr155. On the other hand, Wang4 possessed hydrogen bond interaction with Arg66 and Glu111. The conformation of Wang4 was stabilized by the presence of π - π as well as π -cation interaction between one phenyl ring of the ligand with Tyr155 and Lys15, respectively. Either Wang3 or Wang4 had xanthone like structure, which could be a good lead compounds for further MBP inhibitor associating with its potency as antibacterial against *E. coli*.

In silico activity against protein targets in T47D cell

Likewise, the 27 same ligands were studied in the screening of 10 protein targets in T47D, namely: human placental aromatase CYP450 (PDB 3EQM) [40], human oxydosqualenecyclase (PDB 1W6K) [41], c-src tyrosine kinase (PDB 3G5D) [42], Erb tyrosine kinase (PDB 3BBT) [43], human tubulin cholcicine receptor (PDB 1SAO) [44], estrogen receptor DNA binding protein (PDB 1GWQ) [45], PPR γ nuclear (PDB 1FM6) [46], ER α nuclear receptor (PDB 3ERT) [47], p38 α MAP kinase (PDB 3HEG) [48] and BC1-X1 (PDB 1YS1) [49]. Table 7 presented the docking results of 26 ligands against diverse protein targets in T47D.

Table 7. The $\Delta G_{\text{binding}}$ of 27 ligands were docked into proteins in & T47D cell lines

Ligands	ΔG_{bind} (Kcal/mol) samples (mean \pm SD) <i>n</i> = 10 experiments	1SAO	1W6K	3BBT	3EQM	3G5D	1GWQ	1FM6	3ERT	3HEG	1YSI
HWergos	-8.1 \pm 0.98	-11.2 \pm 0.11	-10.7 \pm 0.76	-10.0 \pm 0.65	-8.6 \pm 0.65	-6.4 \pm 0.85	-6.4 \pm 0.85	-7.5 \pm 0.65	-5.8 \pm 0.76	-7.8 \pm 0.98	-7.6 \pm 0.98
HWergos58	-8.0 \pm 0.65	-9.1 \pm 0.13	-8.4 \pm 0.55	-9.7 \pm 0.99	-8.4 \pm 0.89	-6.4 \pm 0.86	-6.4 \pm 0.86	-7.9 \pm 0.99	-5.7 \pm 0.43	-6.9 \pm 0.85	-7.9 \pm 0.87
Latef1	-8.6 \pm 0.87	-10.1 \pm 0.46	-8.9 \pm 0.63	-9.3 \pm 0.12	-9.3 \pm 0.75	-8.9 \pm 0.98	-8.1 \pm 0.73	-8.8 \pm 0.54	-8.8 \pm 0.77	-8.0 \pm 0.77	-8.6 \pm 0.94
Latef2	-4.8 \pm 0.45	-4.9 \pm 0.63	-4.6 \pm 0.87	-5.8 \pm 1.23	-4.2 \pm 0.43	-4.7 \pm 0.53	-4.3 \pm 0.54	-4.8 \pm 0.76	-4.8 \pm 0.76	-4.6 \pm 0.76	-4.5 \pm 0.48
Latef3	-5.3 \pm 0.37	-5.7 \pm 0.46	-5.1 \pm 0.88	-5.6 \pm 0.35	-4.7 \pm 0.78	-5.5 \pm 0.65	-4.8 \pm 0.48	-5.7 \pm 0.77	-4.8 \pm 0.47	-4.8 \pm 0.47	-5.1 \pm 0.99
Latef4	-8.7 \pm 0.37	-11.3 \pm 0.56	-9.5 \pm 0.97	-9.8 \pm 0.62	-9.8 \pm 0.66	-8.1 \pm 0.77	-7.9 \pm 0.47	-7.3 \pm 0.83	-7.3 \pm 0.83	-8.3 \pm 0.85	-9.6 \pm 0.32
Latef5	-8.5 \pm 0.77	-11.0 \pm 0.66	-9.2 \pm 0.13	-9.6 \pm 0.98	-8.8 \pm 0.62	-8.4 \pm 0.84	-7.8 \pm 0.49	-7.5 \pm 0.99	-7.5 \pm 0.99	-8.4 \pm 0.85	-9.4 \pm 0.66
Latef6	-8.8 \pm 0.98	-10.3 \pm 0.68	-9.0 \pm 0.53	-8.8 \pm 0.77	-9.0 \pm 0.98	-8.7 \pm 0.57	-7.9 \pm 0.77	-8.4 \pm 0.98	-8.4 \pm 0.98	-8.0 \pm 0.21	-8.8 \pm 0.53
Marwah1	-8.0 \pm 0.59	-9.9 \pm 0.31	-8.8 \pm 0.74	-8.3 \pm 0.64	-7.7 \pm 0.88	-6.0 \pm 0.88	-7.2 \pm 0.92	-6.7 \pm 0.83	-6.7 \pm 0.83	-7.5 \pm 0.74	-9.3 \pm 0.75
Marwah2	-7.4 \pm 0.37	-10.6 \pm 0.44	-6.9 \pm 0.77	-8.6 \pm 0.88	-7.3 \pm 0.43	-5.6 \pm 0.72	-7.3 \pm 0.47	-5.8 \pm 0.76	-5.8 \pm 0.76	-6.8 \pm 0.64	-8.2 \pm 0.87
Marwah3	-8.1 \pm 0.87	-3.1 \pm 0.35	-5.8 \pm 0.98	-9.5 \pm 0.82	-8.0 \pm 0.88	-2.0 \pm 0.68	-7.5 \pm 0.83	-1.1 \pm 0.53	-1.1 \pm 0.53	-6.3 \pm 0.42	-3.1 \pm 0.74
Marwah4	-6.9 \pm 0.98	-4.4 \pm 0.51	-8.5 \pm 0.91	-11.3 \pm 0.76	-8.0 \pm 0.43	-1.1 \pm 0.98	-8.0 \pm 0.77	-1.2 \pm 0.65	-1.2 \pm 0.65	-7.0 \pm 0.89	-2.8 \pm 0.86
Marwah5	-6.0 \pm 0.57	-7.8 \pm 0.47	-6.8 \pm 0.65	-6.4 \pm 0.85	-6.2 \pm 0.83	-5.8 \pm 0.92	-5.6 \pm 0.82	-6.3 \pm 0.77	-6.3 \pm 0.77	-6.6 \pm 0.66	-7.0 \pm 0.42
Marwah6	-6.0 \pm 0.98	-8.0 \pm 0.55	-6.0 \pm 0.66	-6.7 \pm 0.44	-5.9 \pm 0.76	-6.0 \pm 0.68	-5.0 \pm 0.39	-6.4 \pm 0.97	-6.4 \pm 0.97	-6.7 \pm 0.86	-6.2 \pm 0.46
Marwah7	-5.2 \pm 0.54	-10.2 \pm 0.73	-7.9 \pm 0.89	-8.4 \pm 0.32	-8.1 \pm 0.77	-6.4 \pm 0.64	-6.9 \pm 0.46	-7.2 \pm 0.86	-7.2 \pm 0.86	-6.8 \pm 0.74	-7.0 \pm 0.87
PengLi	-5.3 \pm 0.49	-6.5 \pm 0.87	-5.9 \pm 0.99	-5.6 \pm 0.94	-6.0 \pm 0.86	-5.9 \pm 0.58	-5.1 \pm 0.74	-6.1 \pm 0.89	-6.1 \pm 0.89	-5.7 \pm 0.89	-6.1 \pm 0.88
Qim1	-0.6 \pm 0.72	-8.7 \pm 0.81	-9.2 \pm 0.42	-9.9 \pm 0.64	-9.3 \pm 0.46	-6.5 \pm 0.88	-8.6 \pm 0.68	-6.2 \pm 0.66	-6.2 \pm 0.66	-8.3 \pm 0.76	-9.5 \pm 0.45
Qim2	0.8 \pm 0.56	-8.5 \pm 0.67	-9.1 \pm 0.64	-9.7 \pm 0.77	-9.2 \pm 0.67	-5.3 \pm 0.94	-8.8 \pm 0.85	-6.1 \pm 0.42	-6.1 \pm 0.42	-8.3 \pm 0.43	-9.5 \pm 0.55
Qim3	-3.5 \pm 0.47	-3.1 \pm 0.82	-9.4 \pm 0.91	-10.0 \pm 0.85	-9.4 \pm 0.53	-6.9 \pm 0.95	-7.9 \pm 0.83	-8.7 \pm 0.52	-8.7 \pm 0.52	-10.3 \pm 0.5	-9.4 \pm 0.75
Qim4	8.8 \pm 0.73	-2.3 \pm 0.44	-10.4 \pm 0.65	-9.1 \pm 0.78	-9.7 \pm 0.24	-5.7 \pm 0.45	-9.0 \pm 0.57	-6.9 \pm 0.68	-6.9 \pm 0.68	-10.4 \pm 0.7	-9.7 \pm 0.87
Wang1	-6.9 \pm 0.84	-10.4 \pm 0.87	-8.5 \pm 0.76	-9.4 \pm 0.96	-9.1 \pm 0.36	-6.5 \pm 0.87	-7.7 \pm 0.52	-5.5 \pm 0.75	-5.5 \pm 0.75	-8.2 \pm 0.64	-8.7 \pm 0.86
Wang2	-5.8 \pm 0.05	-10.0 \pm 0.84	-9.3 \pm 0.77	-9.1 \pm 0.82	-9.7 \pm 0.46	-5.7 \pm 0.98	-8.1 \pm 0.83	-6.3 \pm 0.64	-6.3 \pm 0.64	-8.1 \pm 0.86	-9.4 \pm 0.32
Wang3	-8.4 \pm 0.73	-9.8 \pm 0.99	-8.5 \pm 0.93	-8.0 \pm 0.56	-8.6 \pm 0.66	-8.4 \pm 0.67	-7.2 \pm 0.84	-8.7 \pm 0.55	-8.7 \pm 0.55	-8.2 \pm 0.66	-8.6 \pm 0.65
Wang4	-8.4 \pm 0.57	-9.8 \pm 0.75	-8.8 \pm 0.45	-8.1 \pm 0.81	-8.7 \pm 0.47	-7.9 \pm 0.84	-7.2 \pm 0.83	-8.2 \pm 0.31	-8.2 \pm 0.31	-8.4 \pm 0.53	-8.6 \pm 0.76
Wang5	-6.8 \pm 0.76	-8.2 \pm 0.50	-6.7 \pm 0.65	-6.8 \pm 0.22	-7.0 \pm 0.37	-7.0 \pm 0.89	-6.0 \pm 0.87	-7.0 \pm 0.74	-7.0 \pm 0.74	-7.0 \pm 0.68	-7.1 \pm 0.87
WPI1	5.6 \pm 0.86	3.8 \pm 0.63	-6.6 \pm 0.72	-8.9 \pm 0.46	-7.2 \pm 0.36	-3.9 \pm 0.99	-7.4 \pm 0.83	-4.1 \pm 0.52	-4.1 \pm 0.52	-7.1 \pm 0.77	-3.6 \pm 0.88
WPI2	7.9 \pm 0.54	7.7 \pm 0.77	-7.2 \pm 0.77	-8.9 \pm 0.71	-6.3 \pm 0.48	-3.8 \pm 0.24	-7.8 \pm 0.65	-4.1 \pm 0.67	-4.1 \pm 0.67	-7.4 \pm 0.86	-5.9 \pm 0.98
Mean	-4.8 \pm 0.25	-7.2 \pm 0.52	-8.0 \pm 0.32	-8.6 \pm 0.62	-7.9 \pm 0.66	-6.1 \pm 0.54	-7.2 \pm 0.84	-6.3 \pm 0.88	-6.3 \pm 0.88	-7.5 \pm 0.68	-7.5 \pm 0.93

ΔG_{bind} : Free energy of binding, 1SAO: Human tubulin cholicline receptor, 1W6K: Human oxydosalenecyclase, 3BBT: Erb tyrosine kinase, 3EQM: Human placental aromatase, 3G5D: C-src tyrosine kinase, 1GWQ: Estrogen receptor DNA binding protein, 1FM6: PPRy nuclear, 3ERT: ER α nuclear receptor, 3HEG: P38 α MAP kinase, 1YSI: BCL-XL

Likewise, the range of ΔG_{bind} for predicting active ligands against 10 protein targets in T47D was at -11.3 to -4.2 kcal/mol, whereas predicted inactive ligands were at -2.8 to 8.8 kcal/mol. Overall proteins, human placental aromatase CYP450 (PDB 3EQ) was identified having the lowest value in the mean of ΔG_{bind} among all 27 ligands. This indicated its potential as the protein target in blocking T47D cell growth. Human placental aromatase is an integral membrane enzyme, which catalyzes the demethylation and aromatization of androgen, which is a precursor to synthesize human estrogen [50]. Estrogen is the primary messenger in control of breast cancer, thereby inhibition of human aromatase is one of multiple ways to degenerate the breast cancer cell replication. Table 8 presented the amino acid residues involved in the binding of 27 ligands-human aromatase.

Table 8. The amino acid residues identified from the interaction of 27 ligands with 3EQM

Ligands	Amino acid residues	Lig ands	Amino acid residues
Control	Met374	Marwah6	Ile133, Arg115, Trp141, Arg145, Arg435
HWergos	Leu372	Marwah7	Ala438, Gly439
HWergos58	Met374	PengLi	No H-bond
Latef1	Arg115, Arg435	Qin1	Arg115
Latef2	Arg115, Trp141, Arg145, Arg435	Qin2	Arg115, Thr310
Latef3	Arg115, Arg435, Ala438	Qin3	No H-bond
Latef4	Ile132, Arg115, Arg435	Qin4	No bond
Latef5	Arg115, Arg435	Wang1	Ala438
Latef6	Arg115, Arg435	Wang2	Ala438
Marwah1	Thr310	Wang3	Met374
Marwah2	No H-bond	Wang4	Met374
Marwah3	Arg115, Ser314	Wang5	No bond
Marwah4	Arg115, Ser314	WP1	Arg115, Met374
Marwah5	No H-bond	WP2	Ile133, Arg115, Arg435

3EQM: Human placental aromatase, Met: Methionine, Leu: Leucine, Arg: Arginine, Trp: Tryptophan, Ala: Alanine, Ile: Isoleucine, Thr: Threonine, Ser: Serine, Gly: Glycine, Met: Methionine, No H-bond: No hydrogen bond

The control ligand (4-androstene-3-17-dione) only showed one hydrogen bond interaction with Met374. The major contributor in this ligand-protein interaction was hydrophobic character of steroid scaffold surrounded by non-polar amino acid residues such as Ile133 and Leu477. Four ligands: HWergos58, Wang3, Wang4 and WP1 demonstrated the similar pose with the control ligand due to their interactions with Met374 via hydrogen bonding. It was not surprising that HWergos58 had a similar pose with the control ligand since they beard same steroid-based scaffold. Ligand WP1 possesses one extra hydrogen bond interaction with Arg115. Surprisingly, Wang3 and Wang4 which previously hits as MBP inhibitor, also demonstrated a strong interaction with human aromatase indicated that their potential to be both antibacterial as well as anticancer. Overall, all ligands indicated their potencies as lead compounds for further optimization as human aromatase inhibitors. Two other ligands, i.e., Marwah6 and WP2 showed hydrogen bond interactions with Ile133 indicating the hydrophobic interactions with the corresponding amino acid residue were strengthened by the presence of such hydrogen bonds. Five ligands (Marwah2, Marwah5,

PengLi, Qin3, Qin4 and Wang5) had no hydrogen bond interaction with the aromatase, however they still occupied the binding site via hydrophobic interaction. Figure 5 illustrated the superposition of 27 ligands at the binding site of the human aromatase and the most active ligand-aromatase molecular interaction.

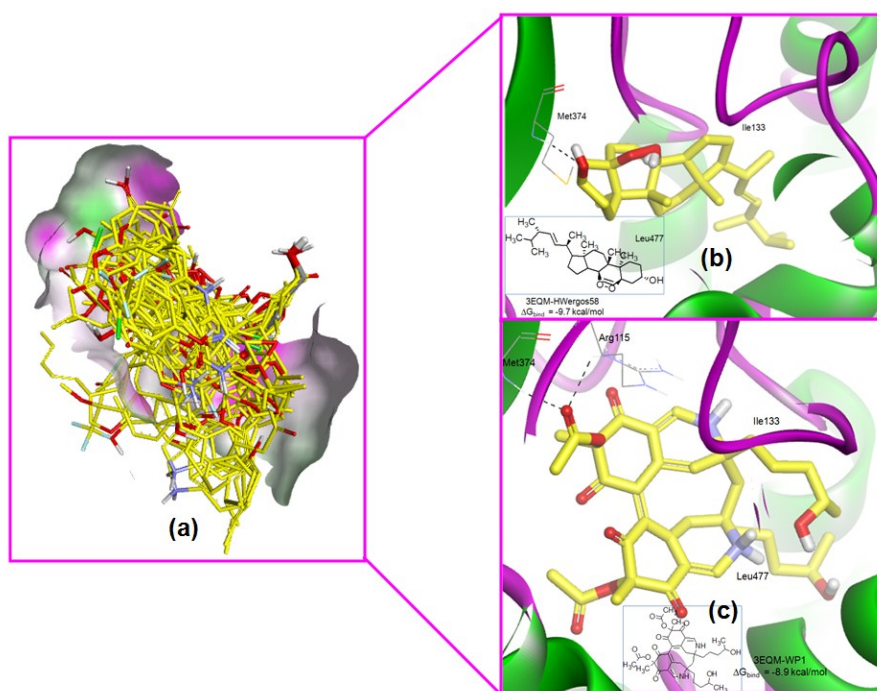


Figure 5. The superposition of (a) 27 ligands in *Chaetomium* sp., the pose of (b) HWergos58, and (c) HP1 at the binding site of 3EQM. The individual poses of HWergos58 and HP1 was visualized as stick forms with carbon in yellow and standard colors of O and H whereas the protein was performed as ribbon, whereas the superposition was as surface. The protein was colored representing green as hydrogen bond acceptor (HB, magenta as hydrogen bond donor (HBD) and white as neutral region. The picture was visualized using Discovery Studio 3.5 (www.accelrys.com)

CONCLUSION

Fungal Endophyte of *Chaetomium* sp. genus isolated from *Phyllanthus niruri* in organic fractions such as *n*-hexane, dichloromethane and ethanol was studied its various biological activities as antimicrobial, antioxidant and cytotoxic agent against breast cancer cell. Dichloromethane was selected as the most active fractions inhibiting the representative bacteria cell growth and T47D breast cancer cell lines, whereas ethanol 96% was found as the most active antioxidant. It was observed that *E. coli* was the most sensitive bacteria against the dichloromethane fraction. In this study, we have a limitation in isolating and characterizing compounds, which is contained in fungal endophyte of *Phyllanthus niruri*. On the other hand, we also have a limitation in testing the activity of the fractions against *E. coli* and T47D breast cancer cell lines at enzyme or receptor level, affecting our limitation to study the molecular mechanism of the fungal endophyte from *Phyllanthus niruri* as antibacterial as well as anticancer. However, we initiated to study the molecular mechanism of some representatives compounds reported in *Chaetomium* sp. against diverse protein targets in *E. coli* as well as T47D breast cancer cell lines to guide our further experiment in

isolating compounds from the corresponding endophyte and test them against the selected protein targets. The docking studies showed that compounds bearing xanthone structure were potential for maltose binding periplasmic and human aromatase associated with their potencies as antibacteria and anticancer, respectively. Beside, compounds bearing steroid is also potential for human aromatase inhibitor due to it is disclose scaffold with the control ligand of human aromatase. We are ongoing to isolate the compounds from the endophyte thus hoping that this preliminary docking simulation could make the isolation of active compounds being more guided.

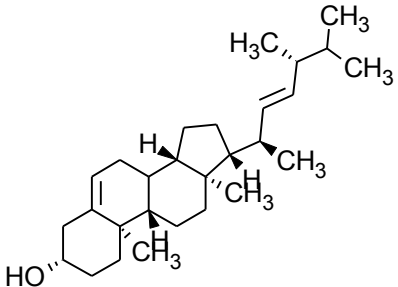
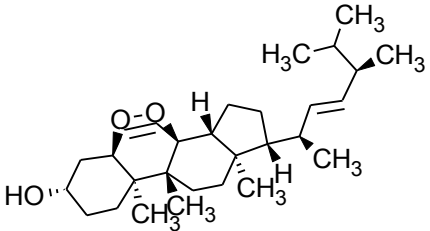
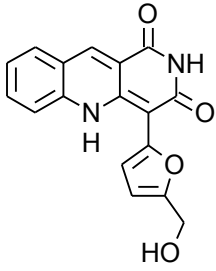
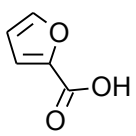
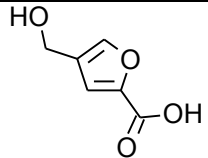
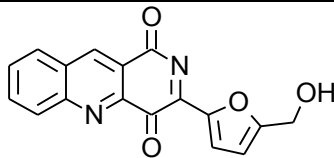
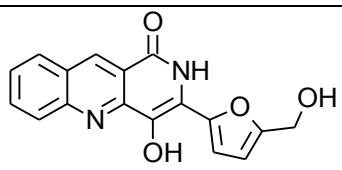
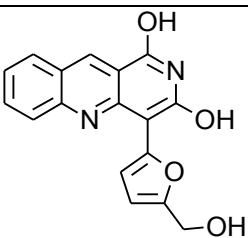
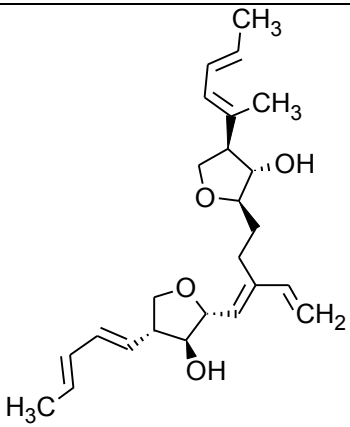
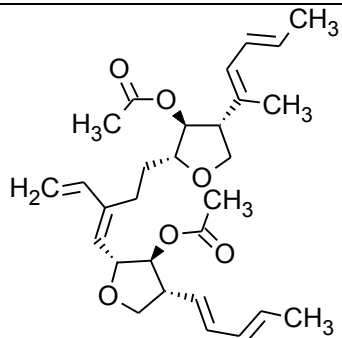
REFERENCES

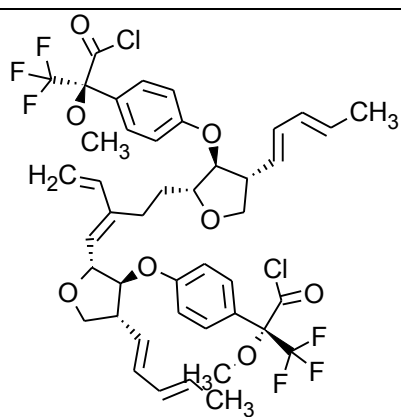
- [1] Strobel, G.A., *Microb Infect*, **2003**, 5(6), 535-544.
- [2] Tanaka, M., Sukiman, H., Takebayashi, M., Saito, K., Suto, M., Prana, T. K., Prana, M. S., Tomita, F., *Microbes Environ*, **1999**, 14(4), 237-241.
- [3] Ruch, R.J., S. Cheng, and J. E. Klaunig, *Carcinogenesis*, **1989**, 10(6), 1003-1008.
- [4] Kandavel, D. and S. Sekar, *Int J Pharm Pharm Sci*, **2015**, 7(5), 253-257.
- [5] Sowparthani, K. and G. Kathiravan, *J Pharm Biomed Sci.*, **2011**, 10(10), 1-10.
- [6] Paithankar V. V., Raut K. S., Charde R. M., Vyas J. V., *Res. Pharm.*, **2015**, 1(4), 1-9.
- [7] Colpo, E., Vilanova, C. D. D. A., Pereira., R. P., Reetz, L. G. B., Oliveira, L., Farias, I. L. G., Boligon, A. A., Athayde, M. L., Rocha, J. B. T., *Asian Pac J Trop Med.*, **2014**, 7(2), 113-118.
- [8] Mediani, A., Abas, F., Khatib, A., Tan, C. P., Ismail, I. S., Lajis, N. H., *Plant Foods Hum Nutr*, **2015**, 70(2), 184-192.
- [9] Sies, H., *Exp Physiol*, **1997**, 82(2), 291-295.
- [10] Mans, D. R., A. B. Da Rocha, and G. Schwartzmann, *Oncologist*, **2000**, 5(3), 185-198.
- [11] Hudzicki, J., *Am Soc Microbiol*, **2009**, 1-23.
- [12] Schwarz, S., Silley, P., Simjee, S., Woodford, N., Duijkeren, E. v., Johnson, A. P., Gastra, W., *J Antimicrob Chemother*, **2010**, 65(4), 601-604.
- [13] Bressan, W. and M. T. Borges, *BioControl*, **2004**, 49(3), 315-322.
- [14] Singleton, V. L. and J. A. Rossi, *Am J Enol Vitic*, **1965**, 16(3), 144-158.
- [15] Oyaizu, M., *Jpn J Nutr*, **1986**, 44, 307-315.
- [16] Hayon, T., Dvilansky, A., Shpilberg, O., and Nathan, I., *Leuk Lymphoma*, **2003**, 44(11), 1957-1962.
- [17] Sharma, O.P., *Textbook of Fungi*. **1989**, Tata McGraw-Hill.
- [18] Ares, M., Bacterial RNA isolation, *Cold Spring Harb Protoc*, **2012**, 2012(9), 1024-1027.
- [19] Karey, K.P. and D.A. Sirbasku, *Cancer Res*, **1988**, 48(14), 4083-4092.
- [20] Baars, L., Protein targeting, translocation and insertion in Escherichia coli: Proteomic analysis of substrate-pathway relationships, **2007**, Stockholms Universitet, Sweden.
- [21] Abdel-Lateff, A., *Tetrahedron Lett*, **2008**, 49(45), 6398-6400.
- [22] Marwah, R. G., Fatope, M. O., Deadman, M. L., Al-Maqbali, Y. M., Husband, J., *Tetrahedron*, **2007**, 63(34), 8174-8180.
- [23] Li, P., Yang, G., Qiu, Y., Lin, L., Dong, F., *Phytochem Lett*, **2015**, 13, 334-342.
- [24] Wang, M. H., Li, L., Jiang, T., Wang, X. -W., Sun, B.-D., Song, B., Zhang, Q.-B., Jia, H. -M., Ding, G., Zou, Z.-M., *Chin Chem Lett*, **2015**, 26(12), 1507-1510.
- [25] Wang, Y., Xu, L., Ren, W., Zhao, D., Zhu, Y., Wu, X., *Phytomedicine*, **2012**, 19(3), 364-368.
- [26] Peng, W., Guo, L., Zheng, C. J., Zhang, Q. Y., Jia, M., Jiang, Y. -P., *Biochem Sys Ecol*, **2012**, 45, 124-126.

- [27] Qin, J. -C., Zhang, Y. -M., Gao, J. -M., Bai, M. -S., Yang, S. -X., *Bioorg Med Chem Lett*, **2009**, 19(6), 1572-1574.
- [28] Kemp, L. E., C. S. Bond, and W. N. Hunter, *Acta Crystallogr Sect D-Biol*, **2003**, 59(3), 607-610.
- [29] Mascarenhas, N. M. and J. Kästner, *Proteins: Struct Funct Bioinf*, **2013**, 81(2), 185-198.
- [30] McKnight, G. L., Mudri, S. L., Mathewes, S. L., Traxinger, R. R., Marshall, S., Sheppard, P. O. and O'Hara, P. J., *J Biol Chem*, **1992**, 267(35), 25208-25212.
- [31] Dover, S. and Halpern, Y. S., *J Bacteriol*, **1972**, 109(2), 835-843.
- [32] Brvar, M., Perdih, A., Renko, M., Anderluh, G., Turk, D., Solmajer, T., *J Med Chem*, **2012**, 55(14), 6413-6426.
- [33] Seefeld, M.A., Miller, W. H., Newlander, K. A., Burgess, W. J., Payne, D. J., Rittenhouse, S. F., Moore, T. D., DeWolf Jr., W. E., Keller, P. M., Qiu, X., Janson, C. A., Vaidya, K., Fosberry, A. P., Smyth, M. G., Jaworski, D. D., Slater-Radosti, C., Huffman, W. F., *Bioorg Med Chem Lett*, **2001**, 11(17), 2241-2244.
- [34] Nakama, T., O. Nureki, and S. Yokoyama, *J Biol Chem*, **2001**, 276(50), 47387-47393.
- [35] Hayashi, H., Mizuguchi, H., Miyahara, I., Nakajima, Y., Hirotsu, K., and Kagamiyama, H., *J Biol Chem*, **2003**, 278(11), 9481-9488.
- [36] Gil-Ortiz, F., Ramón-Maiques, S., Fita, I., Rubio, V., *J Mol Biol*, **2003**, 331(1), 231-244.
- [37] Schmitt, E., Mechulam, Y., Fromant, M., Plateau, P., Blanquet, S., *EMBO J*, **1997**, 16(15), 4760-4769.
- [38] Davidson, A. L., H. A. Shuman, and H. Nikaido, *Proc Natl Acad Sc*, **1992**, 89(6), 2360-2364.
- [39] Patrick, G. L., *An introduction to medicinal chemistry*. **2013**, Oxford university press.
- [40] Ghosh, D., Griswold, J., Erman, M., Pangborn, W., *Nature*, **2009**, 457(7226), 219-223.
- [41] Thoma, R., Schulz-Gasch, T., D'Arcy, B., Benz, J., Aebi, J., Dehmlow, H., Hennig, M., Stihle, M., & Ruf, A., *Nature*, **2004**, 432(7013), 118-122.
- [42] Getlik, M., Grütter, C., Simard, J. R., Klüter, S., Rabiller, M., Rode, H. B., Robubi, A., and Rauh, D., *J Med Chem*, **2009**, 52(13), 3915-3926.
- [43] Qiu, C., Tarrant, M. K., Choi, S. H., Sathyamurthy, A., Bose, R., Banjade, S., Pal, A., Bornmann, W. G., Lemmon, M. A., Cole, P. A., Leahy, D. J., *Structure*, **2008**, 16(3), 460-467.
- [44] Ravelli, R. B. G., Gigant, B., Curmi, P. A., Jourdain, I., Lachkar, S., Sobel, A., Knossow, M., *Nature*, **2004**, 428(6979), 198-202.
- [45] Warnmark, A., Treuter, E., Gustafsson, J., Hubbard, R. E., Brzozowski, A. M., Pike, A. C. W., *J Biol Chem*, **2002**, 277(24), 21862-21868.
- [46] Gampe, R.T., Montana, V. G., Lambert, M. H., Miller, A. B., Bledsoe, R. K., Milburn, M. V., Kliewer, S. A., Willson, T. M., Xu, H. E., *Mol Cell*, **2000**, 5(3), 545-555.
- [47] Shiau, A.K., Barstad, D., Loria, P. M., Cheng, L., Kushner, P. J., Agard, D. A., Greene, G. L., *Cell*, **1998**, 95(7), 927-37.
- [48] Namboodiri, H.V., Bukhtiyarova, M., Ramcharan, J., *Biochemistry*, **2010**, 49(17), 3611-3618.
- [49] Mezzetti, A., Schrag, J. D., Cheong, C. S., Kazlauskas, R. J., *Chem Biol*, **2005**, 12(4), 427-437.
- [50] Ghosh, D., Jiang, W., Lo, J., Egbuta, C., *Steroids*, **2011**, 76(8), 753-758.

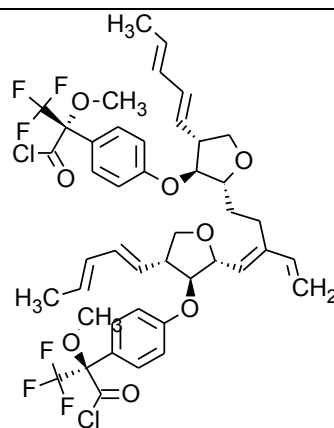
SUPPLEMENTARY DATA

Table 1 : Compounds of *Chaetomium* sp. from diverse plants

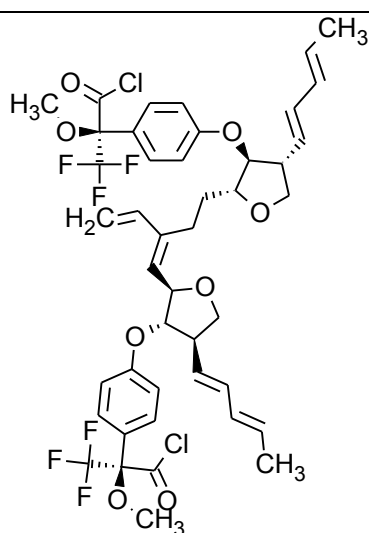
	
HWergos	HWergos58
	
Latef1	Latef2
	
Latef3	Latef4
	
Latef5	Latef6
	
Marwah1	Marwah2



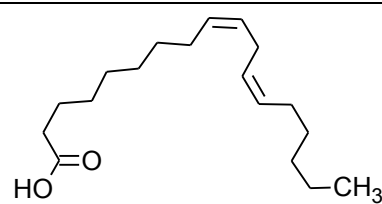
Marwah3



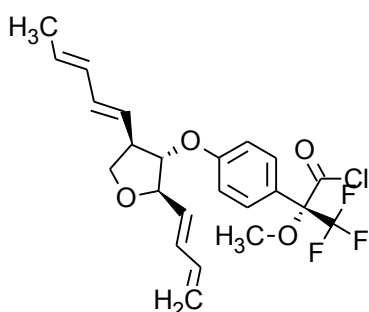
Marwah4



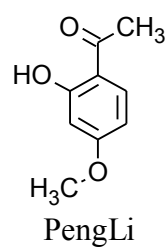
Marwah5



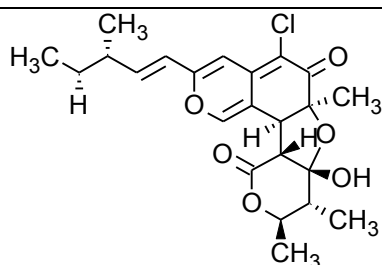
Marwah6



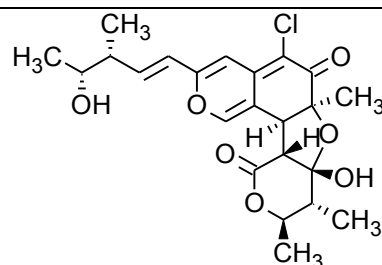
Marwah7



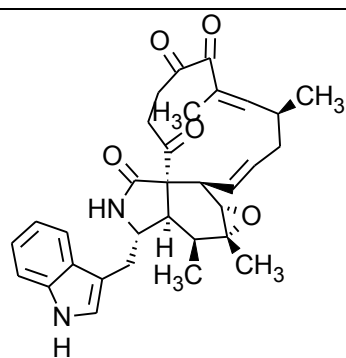
PengLi



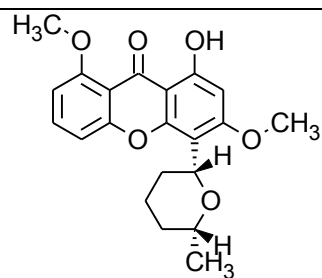
Qin1



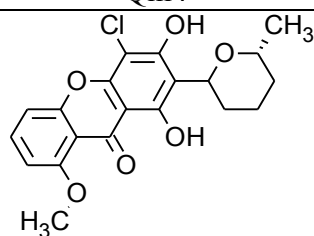
Qin2



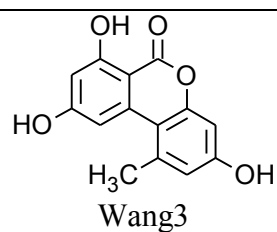
Qin4



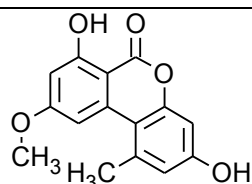
Wang1



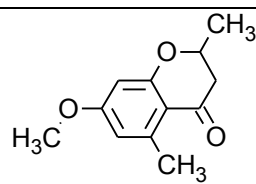
Wang2



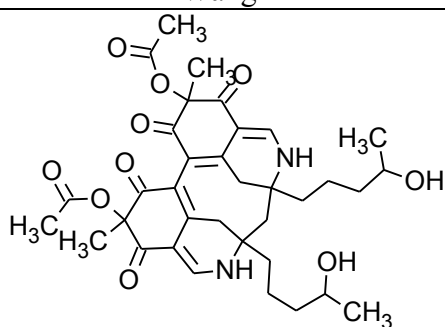
Wang3



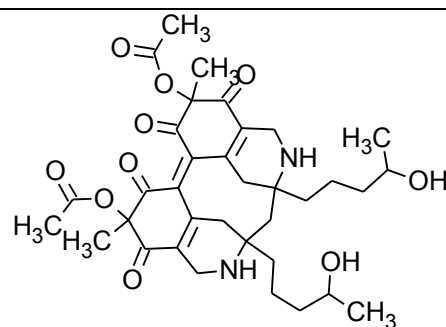
Wang4



Wang5



WP1



WP2